Correlation of the electrophysiological profiles and sodium channel transcripts of individual rat dorsal root ganglia neurons

*Olivier Thériault and Mohamed Chahine **

Department of Medicine, Centre de Recherche de l'Institut Universitaire en Santé Mentale de Québec, Université Laval, Quebec City, QC, Canada

Voltage gated sodium channels (Na$_v$ channels) play an important role in nociceptive transmission. They are intimately tied to the genesis and transmission of neuronal firing. Five different isoforms (Na$_v$1.3, Na$_v$1.6, Na$_v$1.7, Na$_v$1.8, and Na$_v$1.9) have been linked to nociceptive responses. A change in the biophysical properties of these channels or in their expression levels occurs in different pathological pain states. However, the precise involvement of the isoforms in the genesis and transmission of nociceptive responses is unknown. The aim of the present study was to investigate the synergy between the different populations of Na$_v$ channels that give individual neurons a unique electrophysical profile. We used the patch-clamp technique in the whole-cell configuration to record Na$_v$ currents and action potentials from acutely dissociated small diameter DRG neurons ($<30\,\mu$m) from adult rats. We also performed single cell qPCR on the same neurons. Our results revealed that there is a strong correlation between Na$_v$ currents and mRNA transcripts in individual neurons. A cluster analysis showed that subgroups formed by Na$_v$ channel transcripts by mRNA quantification have different biophysical properties. In addition, the firing frequency of the neurons was not affected by the relative populations of Na$_v$ channel. The synergy between populations of Na$_v$ channel in individual small diameter DRG neurons gives each neuron a unique electrophysiological profile. The Na$_v$ channel remodeling that occurs in different pathological pain states may be responsible for the sensitization of the neurons.

Keywords: voltage-gated sodium channel, neuronal excitability, pain, biophysical properties, dorsal root ganglia neurons

INTRODUCTION

Voltage gated sodium channels (Na$_v$ channels) play an important role in nociceptive transmission and are intimately tied to the genesis and transmission of neuronal action potentials. Five isoforms (Na$_v$1.3, Na$_v$1.6, Na$_v$1.7, Na$_v$1.8, and Na$_v$1.9) have been linked to nociceptive responses (Laird et al., 2002; Dib-Hajj et al., 2009; Xie et al., 2013; Garrison et al., 2014). The diversity of the biophysical properties and expression patterns of Na$_v$ channels point to functional specialization (Hu et al., 2009). Moreover, previous studies emphasized the importance of different properties of Na$_v$ in the neuronal excitability. For instance, the slow closed-state inactivation of Na$_v$1.7 is thought to play an important role in the amplification of subthreshold depolarization and initiate AP firing in neurons (Blair and Bean, 2002; Cummins et al., 2007). The fast recuperation from the inactivated state of Na$_v$1.8 is thought to sustain the relatively high frequency firing of small DRG neurons (Cummins and Waxman, 1997; Renganathan et al., 2001) while the current induced by the hyperpolarized activation of Na$_v$1.9 could modulate the membrane voltage and alter the neuronal excitability (Herzog et al., 2001).

Furthermore, defect in biophysical properties of peripheral Na$_v$ channels lead to diverse pain syndromes. Two inherited human neuropathic pain conditions, erythermalgia (Black et al., 2004) and paroxysmal extreme pain disorder (PEPD) (Fertleman et al., 2006), are associated with various missense (gain of function) mutations in SCN9A, the gene encoding the human Na$_v$1.7 channel. PEPD is associated with defective fast inactivation, whereas erythermalgia is associated with a negative-shifted voltage-dependence of activation of Na$_v$1.7 channels (Estacion et al., 2008). More recently, a remarkable congenital indifference to pain (CIP) (Ahmad et al., 2007) was described in consanguineous Pakistani and Canadian individuals, who are homozygous for a null mutation (complete loss of function) of Na$_v$1.7 (Cox et al., 2006; Ahmad et al., 2007). It has also been reported that humans can harbor single nucleotide polymorphisms in SCN9A, which apparently confer different thresholds for pain susceptibility, depending on the functionality of the inherited alleles (Reimann et al., 2010). A variant of Na$_v$1.8 has been reported in a family with painful peripheral neuropathy (Faber et al., 2012). Gain-of-functions mutations on Na$_v$1.9 were reported to induce either loss of pain (Leipold et al., 2013) or episodic pain (Zhang et al., 2013).

The regulation of Na$_v$ channels in sensory neurons is complex and may be a mechanism for conferring unique biophysical

properties on the neurons (Chahine et al., 2005). Changes in the voltage-dependence, kinetics, and expression of Na$_v$ channel subtypes in several models of nerve injury and inflammation used in pain research have been reported (Gold et al., 1998, 2003; Moore et al., 2002; Black et al., 2004; Gold and Flake, 2005; Thakor et al., 2009). These changes have been shown to induce hyperexcitability in primary afferent neurons (Moore et al., 2002; Song et al., 2003).

The aim of the study was to understand how the different Na$_v$ channel α-subunits present in peripheral neurons interact to modulate neuronal excitability and induce the various electrophysiological profiles seen in these neurons. We hypothesized that individual Na$_v$ paralogs contribute to their different biophysical properties to shape the action potential waveforms and overall excitability of peripheral neurons. Clarifying interactions between Na$_v$ subtypes is an important step toward understanding the development of neuropathic pain, and the maturation and diversifications of neurons.

We used the patch-clamp technique in the whole-cell configuration to record Na$_v$ currents and action potentials from acutely dissociated small diameter DRG neurons from adult rats (<30 μm). We also performed single cell qPCR on the same neurons. We compared Na$_v$ channel transcripts in individual neurons and correlated them to the electrophysiological profiles of the neurons to assess their impact on excitability.

The ratio of the expression of mRNA reflected the proportion of Na$_v$ channels at the membrane of the neurons. Moreover, the ratio of the different Na$_v$ channel subtypes expressed in each neuron conferred a unique electrophysiological profile on the neuron. For instance, compared to the Na$_v$1.8 and Na$_v$1.9 channel subtypes, Na$_v$1.7 channel displayed faster AP kinetics and shorter AP. Moreover, the presence of Na$_v$1.7 decreased the threshold potential and accelerates the rise and the decay of the AP.

MATERIALS AND METHODS

DRG NEURON DISSECTION AND CULTURE

Neurons were isolated from L4-L5 DRG of adult male Sprague–Dawley rats weighting from 250 to 350 g (Wilmington, MA). Briefly, freshly removed ganglia were de-sheathed and enzymatically digested at 37°C for 20 min in DMEM containing 2 mg·ml^{-1} of type 4 collagenase (Worthington Biochemical Corp.). Trypsin (2.5 mg·ml^{-1}, Sigma) was added, and the neurons were incubated for an additional 15 min. The ganglia were then dissociated mechanically by trituration using fire-polished Pasteur pipettes. The cell suspensions were centrifuged for 5 min at 1000 rpm at room temperature. The cell pellets were re-suspended in DMEM containing 4 mg·ml^{-1} of type 2S trypsin inhibitor (Sigma), layered on 7.5% BSA in Dulbecco's phosphate buffered saline (DPBS), and centrifuged at 1000 rpm for 5 min. After removing the supernatant, the pellet containing the neurons was re-suspended in DMEM containing 10% heat-inactivated horse serum and 5% FBS. The neurons were plated on poly-d-lysine-coated dishes and were kept in a 5% CO$_2$ incubator at 37°C. The patch-clamp recordings were performed within 18 h. All experiments were performed according to the guidelines of the Canadian Council on Animal Care and were approved by the Université Laval Animal Care Committee.

WHOLE-CELL PATCH-CLAMP RECORDING

Neurons ranging in diameter from 20 to 30 μm (mean short and long axis) measured using a graduated ocular were selected for recording. Whole-cell Na$_v$ currents in DRG neurons were recorded using an Axopatch 200B (Molecular Devices) with the whole-cell configuration of the patch-clamp technique. pClamp v10 (Molecular Devices) was used for the pulse stimulations and recordings. Currents were filtered at 5 kHz, digitized at 100 kHz using a Digidata 1200 series AD converter (Molecular devices), and stored on a personal computer for later offline analysis. Series resistance was compensated 70–80%. When needed, linear leak current artifacts were removed by online leak subtraction. Capillaries used for electrodes were silanized prior to fashioning to reduce mRNA adsorption. The capillaries were soaked in a 5% (v/v) solution of dimethyldichlorosilane (Sigma) in chloroform for 20 min in a fume hood. They were then sterilized (15 min) and dried (15 min) in an autoclave (Lin et al., 2007). Fire-polished low-resistance electrodes (1 MΩ) were pulled from 8161 glass (Corning) and were coated with Sylgard (Dow-Corning) to minimize pipette capacitance.

AP recordings were obtained from DRG neurons using the whole-cell configuration of the patch-clamp technique. APs were generated by 5-ms, 50–300-pA rectangular current pulse injections followed by a 100-ms interpulse at the holding potential and then a 600-ms pulse. The sequence consisted of at least two recordings of evoked APs before and after the addition of 1 μM TTX.

For whole-cell voltage-clamp recordings, the intracellular pipette solution contained 10 mM NaCl, 140 mM CsF, 1 mM EGTA, and 10 mM HEPES. The pH was adjusted to pH 7.3 with 1 mM CsOH. The external solutions contained, the bath solution contained 35 mM NaCl, 105 mM choline chloride, 3 mM KCl, 1 mM CaCl$_2$, 1.0 mM MgCl$_2$, 10 mM glucose, 10 mM HEPES, and 100 nM CdCl$_2$ to block calcium channels. The pH was adjusted to 7.3 with 1 M NaOH.

For the current-clamp recordings, the intracellular solution contained 122 mM KCl, 10 mM NaCl, 1.0 mM MgCl$_2$, 1.0 mM EGTA, and 10 mM HEPES. The pH was adjusted to 7.3 with 1 M KOH. The extracellular solution contained 154 mM NaCl, 5.6 mM KCl, 2.0 mM CaCl$_2$, 1.0 mM MgCl$_2$, 10 mM glucose, and 8.0 mM HEPES. The pH was adjusted to 7.4 with 1 M NaOH.

RT-qPCR

RNA extraction

We used two-step RT-qPCR to evaluate the mRNA in each DRG neuron tested. After the patch-clamp recording, the neuron was drawn into the recording pipette, expelled into a thin wall PCR tube, and stored in liquid nitrogen until the RT-PCR was performed. The RT-PCR reagents were added directly to the tube.

Total RNA for primer validation and standard curves was extracted from the DRG neurons using TRIZOL® (Invitrogen). RNA integrity was evaluated by ethidium bromide staining of 1% agarose gels. Total RNA was quantified by recording the optical density at 260 and 280 nm.

RT-PCR

RT-PCR was performed using Transcriptor First Strand cDNA Synthesis kits (Roche) according to the supplier's protocol.

Briefly, lysed cells or 1 µg of total RNA was added to 60 pmol random hexamer primer and water was added to bring the volume to 13 µL. The template-primer mixture was denatured for 10 min at 65°C. Reaction buffer, RNase inhibitor (20 U final concentration), DNTP (1 mM each), and Transcriptor Reverse Transcriptase (1 U final concentration) were added to the mixture (20 µL). cDNA was synthesized at 50°C for 1 h. The enzymes were heat-deactivated at 85°C for 2 min. cDNA from DRG was stored at −80°C until used. Single cell qPCR was performed on the same day as the electrophysiological recordings.

qPCR

The qPCR assays were performed using a previously described protocol (Chatelier et al., 2012). Briefly, amplification products were detected with SYBR Green I and a LightCycler® 480 platform (Roche) using the supplier's protocol. Primers were designed using PerlPrimer v1.1.19 (Marshall, 2007). The qPCR samples were run at least in duplicate. A non-template control (NTC) and a positive control for each primer pair were included in each qPCR run. The qPCR conditions were as follows: an initial 7-min step at 95°C to activate the Taq polymerase and 45 cycles of 10 s at 95°C and 10 s at 58°C, followed by a 12-s elongation step at 72°C.

qPCR efficiency was determined using a series of known cDNAs, and the Cq values were plotted against the relative cDNA concentrations. qPCR efficiency was calculated using the slope of the regression line using the following equation: $E = 10^{[-1/slope]}$. The analyses were performed using LightCycler® 480 SW 1.5 software. Quantifications were corrected for efficiency and run-to-run variations were adjusted using a known standard:

$$Normalized\ ratio = \left(\frac{[Target]}{[Reference]}\right)_{sample} \div \left(\frac{[Target]}{[Reference]}\right)_{calibrator}$$

Target represents Cp of sodium channels and reference represents Cp of GAPDH (Gudrun, 2006). This is an efficient and accurate method to compensate for efficiency and run-to-run variations without the need of a standard curve in every run (Bustin, 2004). The specificity of the amplification for each run was monitored by melting curve analysis and was performed immediately following the PCR by continuously reading the fluorescence while slowly heating the reaction mixture from 65 to 95°C.

DATA ANALYSIS

Electrophysiological data were analyzed using a combination of pCLAMP software v10.0 (Molecular Devices), Microsoft Excel, and SigmaPlot 12.0 (Systat Software, Inc.).

Unless otherwise stated, statistical analyses were performed using SAS/STAT software v9.2 (SAS Institute Inc.). The results of Pearson analyses are expressed as coefficients of Pearson (ρ). Values are expressed as means ± s.e.m. When required for clarity, results are expressed as z-scores (z-scores = (x-mean)/SD).

Cluster analyses were performed to identify homogenous subsets of neurons based on the mRNA each subset expressed. mRNA quantifications were entered into the cluster analysis based on a Gaussian mixture model implemented in the R software with the Mclust package (available at http://cran.r-project.org/web/packages/mclust/index.html). Since we did not want to define

a number of a priori subgroups of neurons, we compared the adjustments of different clustering solutions with 1, 2, 3, 4, and 5 clusters using the Bayesian Information Criterion (BIC). The inspection of the BIC values showed that the five-cluster solution worked best. However, given that there were very slight differences between two pairs of clusters, we opted for a three-cluster solution. Each subject was then assigned to a most probable cluster.

RESULTS

qPCR AMPLIFICATION EFFICIENCY AND SINGLE-CELL qPCR VALIDATION

We validated the selectivity of the qPCR reaction using ethidium bromide-stained agarose gels. We observed single bands on the agarose gels, indicating that each primer pair produced one amplicon. The amplicons were validated by sequencing (data not shown). qPCR amplification was assessed using a melting curve analysis to ensure that it gave rise to a single PCR product. We evaluated the efficiency of the qPCR by generating standard curves over a wide range of mRNA copies using serial dilutions of known concentrations of cDNA (Supplement Figure 2A). Each primer pair had an efficiency superior to 1.90 in the 5-log range and was efficient with a low copy number (<100 copies) of mRNA (**Table 1**).

Since the quantification was relative to a reference gene, we verified the stability of the selected gene in individual cell experiments. We selected three references genes that are frequently used in qPCR experiments: GAPDH (Glyceraldehyde 3-phosphate dehydrogenase), ACTB (beta-actin), and PPIA (peptidylprolyl isomerase A). We first determined whether the ratio of the genes was stable in single neurons. Supplement Figures 1A,B show the cell-to-cell variations of the ACTB/GAPDH and PPIA/GAPDH gene ratios, respectively. The variations are expressed as (x-mean)/mean. We observed a marked cell-to-cell variation in the ACTB/GAPDH gene ratio of 59% with a mean error of 34%. The variation in the PPIA/GAPDH gene ratio was generally under 20% with a mean error of 12%. There was little correlation

Table 1 | qPCR primers used.

Gene (protein)	Amplification length (pb)	Primer sequence
SCN3A (Na$_v$1.3)	158	F: 5′-AACGAAAGACGATCAAGACC-3′
		R: 5′-CCAAAGAAACATCAACGATCAG-3′
SCN9A (Na$_v$1.7)	163	F: 5′-GGGAACTTGATCTTTACAGGG-3′
		R: 5′-ACTGATAATCCTTCCACATCTG-3′
SCN10A (Na$_v$1.8)	189	F: 5′-TAGACATGGAGAAGAGGGAC-3′
		R: 5′-TTCAAGCTCCTCAATGACAG-3′
SCN11A (Na$_v$1.9)	196	F: 5′-AAATGATCCTGAAGTGGGTG-3′
		R: 5′-GTAGACGACAACCTTCATTCC-3′
GAPDH	152	F: 5′-AGTATGTCGTGGAGTCTACTG-3′
		R: 5′-GGGAGTTGTCATATTTCTCGT-3′
ACTB	175	F: 5′-AGATCAAGATCATTGCTCCTCC-3′
		R: 5′-AACGCAGCTCAGTAACAGTC-3′
PPIA	160	F: 5′-TTTATCTGCACTGCCAAGAC-3′
		R: 5′-AATTAGAGTTGTCCACAGTCGG-3′

between the *Ct* values for ACTB and GAPDH, indicating that there was a large variation in the amount of mRNA among cells (Supplement Figure 1A). As such, GAPDH and ACTB could not be used as references genes. Supplement Figure 1D shows the correlation between the *Ct* values of GAPDH and PPIA for different cells. The high correlation ($R^2 = 0.98$) and the slope value approaching one indicated that there was a low cell-to-cell variation for these two genes. Since GAPDH levels appeared to be stable in individual neurons, we used GAPDH as a reporter gene in our experiments.

We also ensured that the selectivity and efficiency were conserved in our experimental conditions by quantifying serial 1:1 dilutions (up to 1:32) of mRNA from single cells (Supplement Figure 2A). We observed very good quantification at all dilutions, with an error of less than10%. Every amplification product was monitored with a melting curve to ensure that we had a single amplification product.

RT-PCR is often inefficient and can be a source of error (Stahlberg et al., 2004). The relative quantification of the GAPDH reference gene minimizes the risk of error by reducing the influence of variation in the efficiency of the RT-PCR. We assumed that the efficiency was similar for each gene tested and, as such, that the ratios of the Na_v channel transcripts to the reference gene were similar, regardless the efficiency of the RT-PCR. The small amount of mRNA in a single cell and the small volume may also have induced an error. However, any loss of mRNA could be assumed to be the same for each gene we tested and, as such, would also be also minimized by the relative quantification.

mRNAs REFLECT ELECTROPHYSIOLOGICAL PROPERTIES

The voltage-clamp approach can discriminate between TTX-sensitive and resistant Na_v channels. TTX-sensitive Na_v channels (TTX-S) are completely blocked by TTX at low nM concentrations while TTX-resistant Na_v channels (TTX-R) are insensitive to TTX ($IC_{50} > 40 \mu M$) (Caffrey et al., 1992). **Figure 1A** shows an example of a representative Na_v current recorded from a small neuron before (left) and after (right) the addition of 1 μM TTX. The TTX-R Na_v current was probably due to $Na_v1.8$ and $Na_v1.9$ channels. The TTX-S current-voltage relationship (I/V) curve was obtained by subtracting the I/V-curve of the TTX-R Na_v current from the total Na_v current (**Figure 1B**). **Figure 1C** shows the GV curves of TTX-R current and TTX-s current obtain from data of **Figure 1B** (**Figure 1A**). The proportions of the TTX-S and TTX-R Na_v currents were strongly correlated ($R^2 = 0.92$) with the relative expression of mRNA by the TTX-S and TTX-R Na_v channels (**Figure 1D**). In these experiments $Na_v1.6$ was not quantified due to low levels of transcripts in less than 35% of neurons (16 out of 46 neurons), data not shown. These results are similar to the study by Ho and O'leary where $Na_v1.6$ is 6–8 time less abundant than $Na_v1.7$, $Na_v1.8$, and $Na_v1.9$ (Ho and O'Leary, 2011).

IMPACTS ON AP PROPERTIES

We analyzed the parameters of APs recorded from small diameter DRG neurons in the current-clamp mode and quantified the mRNA in the neurons by single-cell qPCR. Neurons ranging in diameter from 20 to 30 μm exhibited marked differences in sensitivity to TTX. Twenty-one of the 49 neurons were sensitive to

1 μM TTX and exhibited no AP firing. **Figure 2A** shows a typical neuron in which AP firing was resistant to TTX. The left panel of **Figure 2A** show a representative AP recording under control conditions and the right panel shows a representative AP recording in the presence of 1 μM TTX. The protocol is shown in the inset. **Figure 2B** shows a neuron whose AP firing was inhibited by TTX. The left panel shows AP firing prior to the addition of TTX and the right panel show that the firing was abolished after the addition of 1 μM TTX. The first AP was not abolished by TTX.

Table 2 shows Pearson correlations between mRNAs and several biophysical properties of the AP. The correlations are expressed as negative or positive *r* values, which were considered significant at $p < 0.05$ (*$p < 0.05$, **$p < 0.01$). There was a significant correlation between $Na_v1.7$ mRNA and the overshoot, threshold (in mV and in pA), rise time (dV/dT), and time of decay as well as between $Na_v1.8$ and $Na_v1.9$ mRNA and the half AP width (duration of the AP at 50% amplitude), current threshold, and overshoot. There was also a significant correlation between $Na_v1.9$ mRNA and a slowing of the rise and decay of dV/dT.

CLUSTER ANALYSIS

We performed another *post-hoc* analysis of the data by plotting the amounts of mRNA in order to visualize their distributions (**Figure 3A**). $Na_v1.7$ mRNA was plotted against $Na_v1.8$ mRNA in $Na_v1.3$ mRNA-positive (red) and $Na_v1.3$ mRNA-negative cells (blue). We observed a marked difference between the two types of cell, with $Na_v1.3$ mRNA-positive cells expressing more $Na_v1.7$ mRNA than $Na_v1.3$ mRNA-negative cells.

We also performed a cluster analysis to determine whether there were different subgroups of neurons (**Figure 3B**). Interestingly, the cluster analysis revealed that there were three subgroups of neurons that differed in the expression of Na_v channel mRNA. The first subgroup (red) expressed large numbers of TTX-R $Na_v1.8$ and $Na_v1.9$ channels. The second subgroup (orange) made up 8% of all the neurons tested and expressed a combination of TTX-S Na_v channels ($Na_v1.7$) and TTX-R Na_v channels ($Na_v1.8$ and $Na_v1.9$). The third subgroup (green) made up 43% of all the neurons tested and mainly expressed TTX-S $Na_v1.7$ Na_v channels.

We performed statistical analyses to determine whether there were any differences in AP parameters between the subgroups. Results are expressed as z-scores on the y axis (**Figure 3C**). We also performed multiple comparisons when the ANOVA *p*-value was less than 0.05 ($p < 0.05$). We observed significant differences between subgroups 1 and 3 (*) and subgroups 2 and 3 (¤). There was a significant difference between subgroups 1 and 2 vs. subgroup 3 in terms of half AP width, overshoot, current threshold, and maximum dV/dt rise. There was also a significant difference between groups 1 and 3 in terms of dV/dt decay. The **Figure 4** illustrates the AP properties of a representative neurons from each groups.

DISCUSSION

One concern with qPCR is that the amount of amplified mRNA is not proportional to the amount of functional protein (Greenbaum et al., 2003; Maier et al., 2009). We recorded voltage-clamp currents and performed single-cell qPCR to measure the
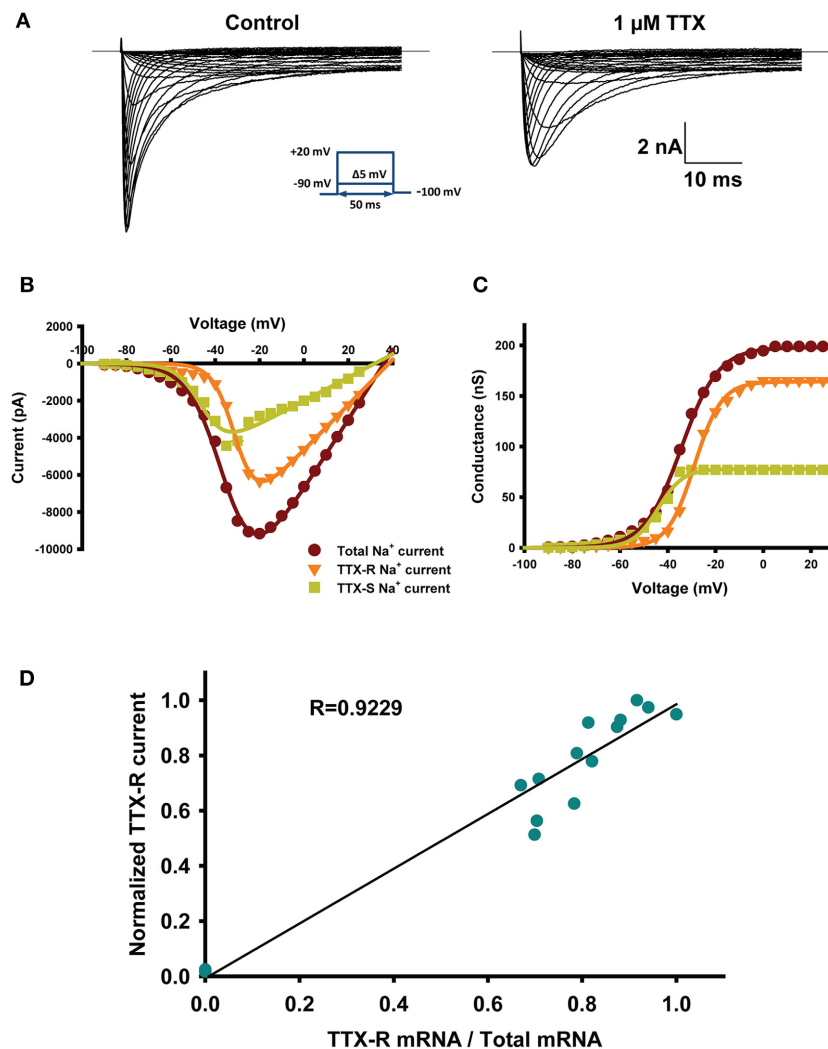
FIGURE 1 | mRNAs reflect electrophysiological properties. (A)
Representative current-traces recorded from small diameter DRG neurons
(28 μm in diameter) before (right) and after (left) the addition of 1 μM TTX.
The protocol is shown in the inset. **(B)** Example of current-voltage (I–V)
relationships obtained from the small diameter DRG neuron shown in **(A)**.
The dark red trace is the total current recorded under control conditions,
the orange trace is the total TTX-R current recorded in presence of 1 μM
TTX, and the green trace is the TTX-S current obtained by subtracting the
TTX-R Na$_v$ current (orange) from the total Na$_v$ current (dark red). I–V are
fitted using a Hodgkin–Huxley-like equation: $f = G_{max} * (V - V_{rev})/$
$(1 + \exp((V - V_{1/2})/k))$, where G_{max} is the maximal conductance, V the

potential, $V_{1/2}$ is the voltage at which half of the channels are in the open
state, V_{rev} is the reversal potential, and k is the slope factor. **(C)** Activation
curves obtained from **(B)** illustrating the conductance of total Na$_v$ current
(dark red), TTX-R current (orange) and TTX-S current (green). The
conductance was calculated using the following equation:
$G_{Na} = I_{Na}/(V_m - V_{rev})$, where G_{Na} is the conductance, I_{Na} is the peak
current for the test potential V_m, and V_{rev} is the reversal potential
estimated from the current-voltage curve. **(D)** Correlation of normalized
TTX-R Na$_v$ currents to normalized mRNA coding for TTX-R channels
(Na$_v$1.8 + Na$_v$1.9/(Na$_v$1.7 + Na$_v$1.8 + Na$_v$1.9)). Currents were normalized to
the maximal current. $n = 17$ from 8 animals.

expression of functional Na$_v$ channels and mRNA (Sucher et al.,
2000; Lin et al., 2007). Adding TTX makes it possible to dis-
criminate between TTX-R and TTX-S Na$_v$ channels and, as such,
correlate the expression of functional TTX-R and TTX-S Na$_v$
channels and their mRNAs. We observed a strong correlation
between the proportion of mRNA and the expression of func-
tional Na$_v$ channels (**Figure 1D**), indicating that the expression
of mRNA was a good representation of the amount of func-
tional protein in our study and could thus be used to quantify
the amount of proteins.

There was a significant correlation between Na$_v$ channel
mRNA and AP parameters. It has been shown that faster Na$_v$
channel kinetics may result in faster AP kinetics (Cummins et al.,
2007; Schild and Kunze, 2012). The presence of Na$_v$1.7 chan-
nels increased the rise in dV/dT, decreased the decay in dV/dT,
and reduced the half AP width of the AP. The correlation anal-
ysis also showed that Na$_v$1.7 channels had a lower threshold
and a higher overshoot than Na$_v$1.8 and Na$_v$1.9 channels while
Na$_v$1.8 and Na$_v$1.9 channels displayed slower AP kinetics than
Na$_v$1.7 channels. This is in agreement with the hypothesis that

FIGURE 2 | Current-clamp analysis. (A) Examples of AP firing (see protocol in inset) recorded from a 27-μm-diameter TTX-R neuron. The left panel shows the recording of AP firing before the addition of TTX, and the right panel shows the recording of AP firing by the same neuron after the addition of 1 μM TTX. **(B)** Examples of AP firing recorded from a 30-μm-diameter TTX-S neuron. The left panel shows the recording of AP firing before the addition of TTX, and the right panel show the recording of AP firing by the same neuron after the addition of 1 μM TTX.
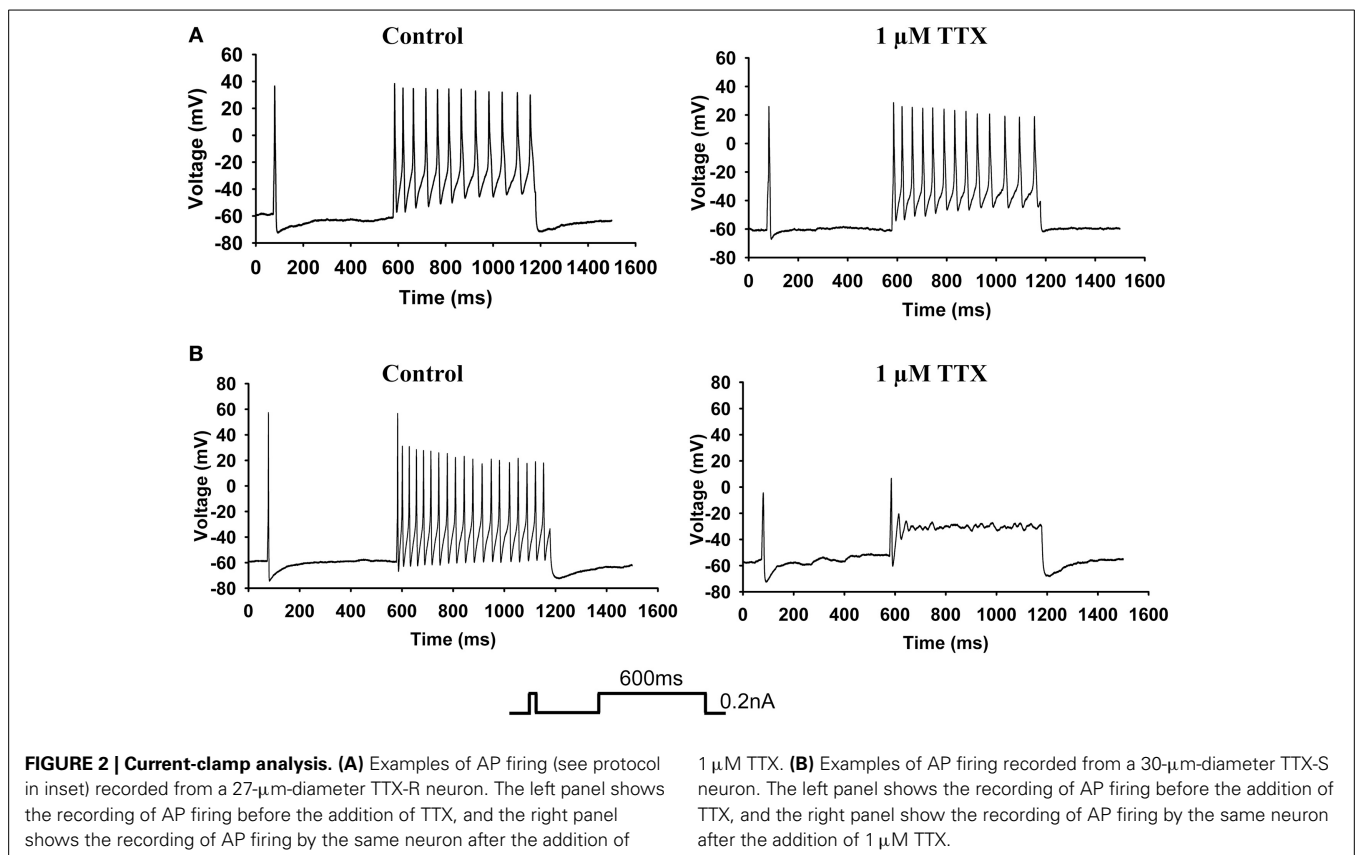
Table 2 | Pearson correlations of Na$_v$ channels mRNA and electrophysiological properties measured.

	Frequency	Half AP width	Overshoot	Threshold (mV)	Threshold (pA)	dV/dT (decay)	dV/dT (rise)
Na$_v$1.7	–	−0.46**	0.43**	−0.32*	−0.46**	−0.30*	0.46**
Na$_v$1.8	–	0.31*	−0.31*	–	0.45**	–	–
Na$_v$1.9	–	0.34*	0.38**	–	0.32*	0.29*	−0.37**

Data are presented as the correlation coefficient of Pearson correlations (ρ). Significant values are presented with *; *p-value < 0.05; **p-value < 0.01; –, no significant correlation.

Na$_v$1.7 amplifies subthreshold stimuli to evoked AP (Blair and Bean, 2002). Moreover, those results can be linked to studies that indicate a role for the upregulation of Na$_v$1.7 in neuropathic pain (Black et al., 2004; Cummins et al., 2004).

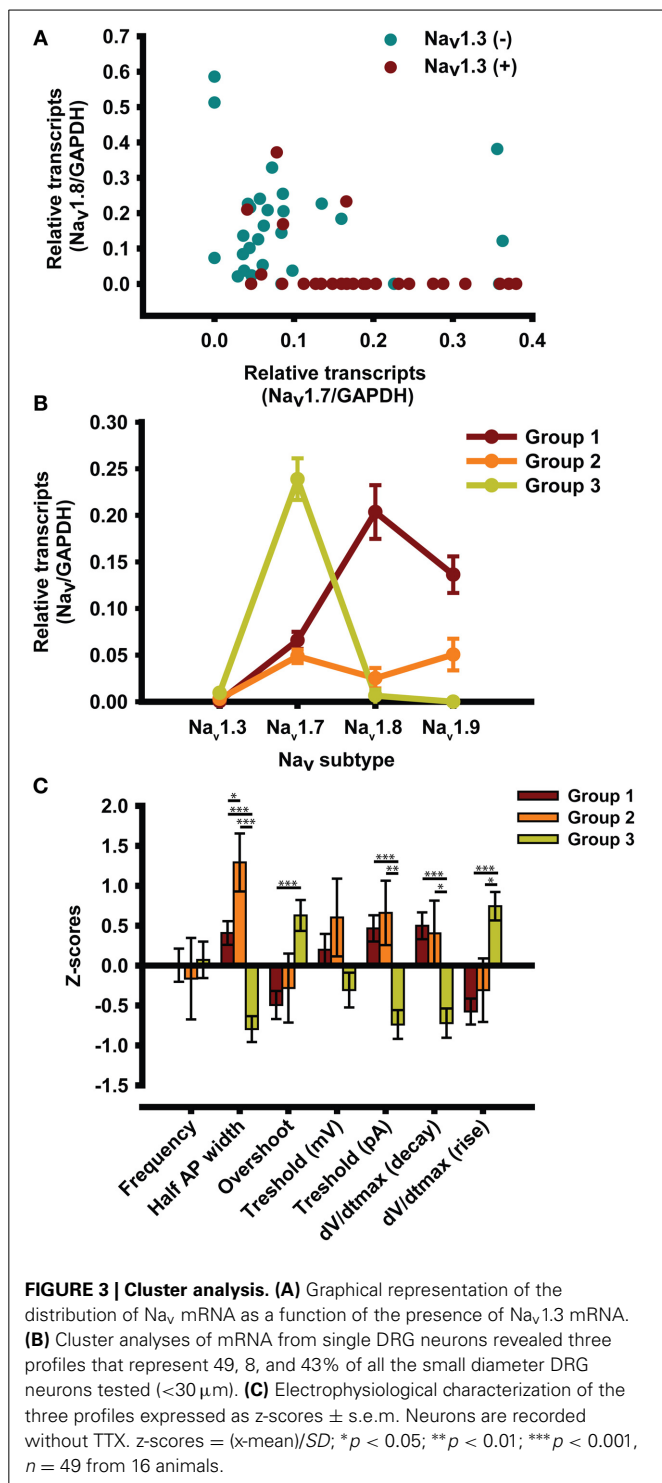In our study, the presence of Na$_v$1.9 and Na$_v$1.8 channels significantly slowed dV/dT rise and decay ($p = 0.06$ for Na$_v$1.9 and $p = 0.05$ for Na$_v$1.8). The half AP width was also correlated with the proportion of Na$_v$1.8 and Na$_v$1.9 Na$_v$ channels, which is in agreement with their slower kinetics (Vijayaragavan et al., 2001). Those results are in accordance with studies which concluded that the sodium channels subtypes have different roles in the electrogenesis within DRG neurons (Rush et al., 2007; Ho and O'Leary, 2011).

Pearson analysis does not show any correlation between Na$_v$ channels transcripts and firing frequency of the neurons (**Table 2**). It has been assumed that slowly inactivating Na$_v$1.8 channels support high frequency firing in small C-fiber neurons
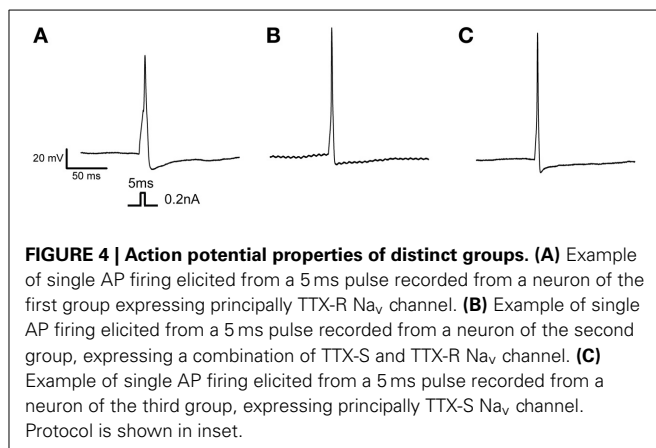
(Renganathan et al., 2001). However, our data showed that both Na$_v$1.7 and Na$_v$1.8 channels can support high frequency tonic firing in DRG neurons. Indeed, Na$_v$1.7 supports high frequency neurons in SCG neurons (Rush et al., 2006).

The plot of the distributions of Na$_v$1.7 and Na$_v$1.8 mRNA showed marked differences depending on whether Na$_v$1.3 mRNA was present or not, which together with prior observations indicated that there are several subtypes of neurons (Fornaro et al., 2008; Ho and O'Leary, 2011). We thus performed a cluster analysis of mRNA distributions, which revealed that there are three subgroups of neurons in small diameter DRG neurons (<30 μm) that we tested. One subgroup mainly expressed Na$_v$1.8 and Na$_v$1.9 mRNA, the second subgroup expressed similar amounts of Na$_v$1.7, Na$_v$1.8, and Na$_v$1.9 mRNA, while the third subgroup mainly expressed Na$_v$1.7 mRNA.

The three subgroups displayed significant differences in AP properties. The frequency and threshold (in mV) were the only

FIGURE 4 | Action potential properties of distinct groups. (A) Example of single AP firing elicited from a 5 ms pulse recorded from a neuron of the first group expressing principally TTX-R Na_v channel. **(B)** Example of single AP firing elicited from a 5 ms pulse recorded from a neuron of the second group, expressing a combination of TTX-S and TTX-R Na_v channel. **(C)** Example of single AP firing elicited from a 5 ms pulse recorded from a neuron of the third group, expressing principally TTX-S Na_v channel. Protocol is shown in inset.

It is interesting that the biophysical properties of the three subgroups were similar to the results of the Pearson correlations. The third subgroup, which had a greater proportion of $Na_v1.7$, had a faster AP, a shorter half AP width, and a faster dV/dT decay and rise than the first and second subgroups. The third subgroup also had a greater overshoot and a lower current threshold than the first and second subgroups. The first and second subgroups, which had more $Na_v1.8$ and $Na_v1.9$ channels than $Na_v1.7$ channels, exhibited slower kinetics than the third subgroup as well as a lower overshoot and a higher current threshold.

Potassium and calcium channels also have a major impact on the firing pattern (Deister et al., 2009; Winlove and Roberts, 2012). It is thus possible that the changes we observed were caused by more than one contributing factor (ion channels, pumps, exchangers, etc.). Nevertheless, the strong linear correlation indicated that Na_v channels play a major role in the biophysical properties of DRG neurons. It's important to keep in mind that electrophysiological properties of a neuron are the results of the equilibrium between the different ion channels present and therefore changes might not lead to the same outcome. As shown by Rush et al., a gain of function mutation of $Na_v1.7$ that lead to erythermalgia render the sensory neurons hyperexcitable and sympathetic neurons hypoexcitable (Rush et al., 2006).

Our results also have major implications during development since the different expression patterns that occur during the maturation of the nervous system (Beckh, 1990) are associated with changes in the electrical excitability of the neurons (Benn et al., 2001). Our results contribute to understanding how the different subtypes of Na_v channels affect the maturation and excitability of sensory neurons.

While there are numerous reports in the literature on the modulation of Na_v channels and the changes in the excitability of sensory neurons during different pathological conditions, little is known about how this affects the excitability of neurons (Cummins and Waxman, 1997; Berta et al., 2008; Thakor et al., 2009). We showed that the modulation of Na_v channels has an impact on the firing properties of acutely dissociated DRG sensory neurons. It now remains to be determined how changes in Na_v channel expression in pathological conditions affect the excitability of neurons.

FIGURE 3 | Cluster analysis. (A) Graphical representation of the distribution of Na_v mRNA as a function of the presence of $Na_v1.3$ mRNA. **(B)** Cluster analyses of mRNA from single DRG neurons revealed three profiles that represent 49, 8, and 43% of all the small diameter DRG neurons tested (<30 μm). **(C)** Electrophysiological characterization of the three profiles expressed as z-scores ± s.e.m. Neurons are recorded without TTX. z-scores = (x-mean)/SD; *$p < 0.05$; **$p < 0.01$; ***$p < 0.001$, $n = 49$ from 16 animals.

parameters that were the same for all three subgroups. The half AP width, overshoot, current threshold, dV/dT decay, and dV/dT rise of the third group differed from those of the first and the second subgroups. The lack of significant differences between the first and second subgroups may be due to the very low proportions of these two subgroup and greater differences between them.

We concluded that the different Na$_v$ channel subtypes in small diameter DRG neurons point to complex physiological interactions and that their modulation affects the biophysical properties of these neurons. Further studies are needed to unravel the roles of the Na$_v$ channel subtypes during development and in pathological conditions.

ACKNOWLEDGMENTS

SUPPLEMENTARY MATERIAL

The Supplementary Material for this article can be found online at: http://www.frontiersin.org/journal/10.3389/fncel.2014.00285/abstract

REFERENCES

Ahmad, S., Dahllund, L., Eriksson, A. B., Hellgren, D., Karlsson, U., Lund, P. E., et al. (2007). A stop codon mutation in SCN9A causes lack of pain sensation. *Hum. Mol. Genet.* 16, 2114–2121. doi: 10.1093/hmg/ddm160

Beckh, S. (1990). Differential expression of sodium channel mRNAs in rat peripheral nervous system and innervated tissues. *FEBS Lett.* 262, 317–322. doi: 10.1016/0014-5793(90)80218-8

Benn, S. C., Costigan, M., Tate, S., Fitzgerald, M., and Woolf, C. J. (2001). Developmental expression of the TTX-resistant voltage-gated sodium channels Na$_v$1.8 (SNS) and Na$_v$1.9 (SNS2) in primary sensory neurons. *J. Neurosci.* 21, 6077–6085.

Berta, T., Poirot, O., Pertin, M., Ji, R. R., Kellenberger, S., and Decosterd, I. (2008). Transcriptional and functional profiles of voltage-gated Na(+) channels in injured and non-injured DRG neurons in the SNI model of neuropathic pain. *Mol. Cell. Neurosci.* 37, 196–208. doi: 10.1016/j.mcn.2007.09.007

Black, J. A., Liu, S., Tanaka, M., Cummins, T. R., and Waxman, S. G. (2004). Changes in the expression of tetrodotoxin-sensitive sodium channels within dorsal root ganglia neurons in inflammatory pain. *Pain* 108, 237–247. doi: 10.1016/j.pain.2003.12.035

Blair, N. T., and Bean, B. P. (2002). Roles of tetrodotoxin (TTX)-sensitive Na$^+$ current, TTX-resistant Na$^+$ current, and Ca^{2+} current in the action potentials of nociceptive sensory neurons. *J. Neurosci.* 22, 10277–10290.

Bustin, S. A. (2004). *A to Z of Quantitative PCR.* La Jolla: International University Line.

Caffrey, J. M., Eng, D. L., Black, J. A., Waxman, S. G., and Kocsis, J. D. (1992). Three types of sodium channels in adult rat dorsal root ganglion neurons. *Brain Res.* 592, 283–297. doi: 10.1016/0006-8993(92)91687-A

Chahine, M., Ziane, R., Vijayaragavan, K., and Okamura, Y. (2005). Regulation of Na(v) channels in sensory neurons. *Trends. Pharmacol. Sci.* 26, 496–502. doi: 10.1016/j.tips.2005.08.002

Chatelier, A., Mercier, A., Tremblier, B., Theriault, O., Moubarak, M., Benamer, N., et al. (2012). A distinct de novo expression of Nav1.5 sodium channels in human atrial fibroblasts differentiated into myofibroblasts. *J. Physiol.* 590, 4307–4319. doi: 10.1113/jphysiol.2012.233593

Cox, J. J., Reimann, F., Nicholas, A. K., Thornton, G., Roberts, E., Springell, K., et al. (2006). An *SCN9A* channelopathy causes congenital inability to experience pain. *Nature* 444, 894–898. doi: 10.1038/nature05413

Cummins, T. R., Dib-Hajj, S. D., and Waxman, S. G. (2004). Electrophysiological properties of mutant Nav1.7 sodium channels in a painful inherited neuropathy. *J. Neurosci.* 24, 8232–8236. doi: 10.1523/JNEUROSCI.2695-04.2004

Cummins, T. R., Sheets, P. L., and Waxman, S. G. (2007). The roles of sodium channels in nociception: implications for mechanisms of pain. *Pain* 131, 243–257. doi: 10.1016/j.pain.2007.07.026

Cummins, T. R., and Waxman, S. G. (1997). Downregulation of tetrodotoxin-resistant sodium currents and upregulation of a rapidly repriming tetrodotoxin-sensitive sodium current in small spinal sensory neurons after nerve injury. *J. Neurosci.* 17, 3503–3514.

Deister, C. A., Chan, C. S., Surmeier, D. J., and Wilson, C. J. (2009). Calcium-activated SK channels influence voltage-gated ion channels to determine the precision of firing in globus pallidus neurons. *J. Neurosci.* 29, 8452–8461. doi: 10.1523/JNEUROSCI.0576-09.2009

Dib-Hajj, S. D., Black, J. A., and Waxman, S. G. (2009). Voltage-gated sodium channels: therapeutic targets for pain. *Pain Med.* 10, 1260–1269. doi: 10.1111/j.1526-4637.2009.00719.x

Estacion, M., Dib-Hajj, S. D., Benke, P. J., Te Morsche, R. H., Eastman, E. M., Macala, L. J., et al. (2008). NaV1.7 gain-of-function mutations as a continuum: A1632E displays physiological changes associated with erythromelalgia and paroxysmal extreme pain disorder mutations and produces symptoms of both disorders. *J. Neurosci.* 28, 11079–11088. doi: 10.1523/JNEUROSCI.3443-08.2008

Faber, C. G., Lauria, G., Merkies, I. S., Cheng, X., Han, C., Ahn, H. S., et al. (2012). Gain-of-function Nav1.8 mutations in painful neuropathy. *Proc. Natl. Acad. Sci. U.S.A.* 109, 19444–19449. doi: 10.1073/pnas.1216080109

Fertleman, C. R., Baker, M. D., Parker, K. A., Moffatt, S., Elmslie, F. V., Abrahamsen, B., et al. (2006). SCN9A mutations in paroxysmal extreme pain disorder: allelic variants underlie distinct channel defects and phenotypes. *Neuron* 52, 767–774. doi: 10.1016/j.neuron.2006.10.006

Fornaro, M., Lee, J. M., Raimondo, S., Nicolino, S., Geuna, S., and Giacobini-Robecchi, M. (2008). Neuronal intermediate filament expression in rat dorsal root ganglia sensory neurons: an *in vivo* and *in vitro* study. *Neuroscience* 153, 1153–1163. doi: 10.1016/j.neuroscience.2008.02.080

Garrison, S. R., Weyer, A. D., Barabas, M. E., Beutler, B. A., and Stucky, C. L. (2014). A gain-of-function voltage-gated sodium channel 1.8 mutation drives intense hyperexcitability of A- and C-fiber neurons. *Pain* 155, 896–905. doi: 10.1016/j.pain.2014.01.012

Gold, M. S., and Flake, N. M. (2005). Inflammation-mediated hyperexcitability of sensory neurons. *Neurosignals* 14, 147–157. doi: 10.1159/000087653

Gold, M. S., Levine, J. D., and Correa, A. M. (1998). Modulation of TTX-R I_{Na} by PKC and PKA and their role in PGE$_2$-induced sensitization of rat sensory neurons *in vitro*. *J. Neurosci.* 18, 10345–10355.

Gold, M. S., Weinreich, D., Kim, C. S., Wang, R., Treanor, J., Porreca, F., et al. (2003). Redistribution of Na$_v$1.8 in uninjured axons enables neuropathic pain. *J. Neurosci.* 23, 158–166.

Greenbaum, D., Colangelo, C., Williams, K., and Gerstein, M. (2003). Comparing protein abundance and mRNA expression levels on a genomic scale. *Genome Biol.* 4:117. doi: 10.1186/gb-2003-4-9-117

Gudrun, T. (2006). The E-Method: a highly accurate technique for gene-expression analysis. *Nat. Methods* 3, i–ii. doi: 10.1038/nmeth894

Herzog, R. I., Cummins, T. R., and Waxman, S. G. (2001). Persistent TTX-resistant Na$^+$ current affects resting potential and response to depolarization in simulated spinal sensory neurons. *J. Neurophysiol.* 86, 1351–1364.

Ho, C., and O'Leary, M. E. (2011). Single-cell analysis of sodium channel expression in dorsal root ganglion neurons. *Mol. Cell Neurosci.* 46, 159–166. doi: 10.1016/j.mcn.2010.08.017

Hu, W., Tian, C., Li, T., Yang, M., Hou, H., and Shu, Y. (2009). Distinct contributions of Na(v)1.6 and Na(v)1.2 in action potential initiation and backpropagation. *Nat. Neurosci.* 12, 996–1002. doi: 10.1038/nn.2359

Laird, J. M. A., Souslova, V., Wood, J. N., and Cervero, F. (2002). Deficits in visceral pain and referred hyperalgesia in Nav1.8 (SNS/PN3)-null mice. *J. Neurosci.* 22, 8352–8356.

Leipold, E., Liebmann, L., Korenke, G. C., Heinrich, T., Giesselmann, S., Baets, J., et al. (2013). A de novo gain-of-function mutation in SCN11A causes loss of pain perception. *Nat. Genet.* 45, 1399–1404. doi: 10.1038/ng.2767

Lin, D. M., Loveall, B., Ewer, J., Deitcher, D. L., and Sucher, N. J. (2007). Characterization of mRNA expression in single neurons. *Methods Mol. Biol.* 399, 133–152. doi: 10.1007/978-1-59745-504-6_10

Maier, T., Guell, M., and Serrano, L. (2009). Correlation of mRNA and protein in complex biological samples. *FEBS Lett.* 583, 3966–3973. doi: 10.1016/j.febslet.2009.10.036

Marshall, O. (2007). Graphical design of primers with PerlPrimer. *Methods Mol. Biol.* 402, 403–414. doi: 10.1007/978-1-59745-528-2_21

Moore, B. A., Stewart, T. M., Hill, C., and Vanner, S. J. (2002). TNBS ileitis evokes hyperexcitability and changes in ionic membrane properties of nociceptive DRG neurons. *Am. J. Physiol Gastrointest. Liver Physiol* 282, G1045–G1051. doi: 10.1152/ajpgi.00406.2001

Reimann, F., Cox, J. J., Belfer, I., Diatchenko, L., Zaykin, D. V., McHale, D. P., et al. (2010). Pain perception is altered by a nucleotide polymorphism in SCN9A. *Proc. Natl. Acad. Sci. U.S.A.* 107, 5148–5153. doi: 10.1073/pnas.0913181107

Renganathan, M., Cummins, T. R., and Waxman, S. G. (2001). Contribution of Na$_v$1.8 sodium channels to action potential electrogenesis in DRG neurons. *J. Neurophysiol.* 86, 629–640.

Rush, A. M., Cummins, T. R., and Waxman, S. G. (2007). Multiple sodium channels and their roles in electrogenesis within dorsal root ganglion neurons. *J. Physiol.* 579, 1–14. doi: 10.1113/jphysiol.2006.121483

Rush, A. M., Dib-Hajj, S. D., Liu, S., Cummins, T. R., Black, J. A., and Waxman, S. G. (2006). A single sodium channel mutation produces hyper- or hypoexcitability in different types of neurons. *Proc. Natl. Acad. Sci. U.S.A.* 103, 8245–8250. doi: 10.1073/pnas.0602813103

Schild, J. H., and Kunze, D. L. (2012). Differential distribution of voltage-gated channels in myelinated and unmyelinated baroreceptor afferents. *Auton. Neurosci.* 172, 4–12. doi: 10.1016/j.autneu.2012.10.014

Song, X. J., Zhang, J. M., Hu, S. J., and LaMotte, R. H. (2003). Somata of nerve-injured sensory neurons exhibit enhanced responses to inflammatory mediators. *Pain* 104, 701–709. doi: 10.1016/S0304-3959(03)00167-2

Stahlberg, A., Hakansson, J., Xian, X., Semb, H., and Kubista, M. (2004). Properties of the reverse transcription reaction in mRNA quantification. *Clin. Chem.* 50, 509–515. doi: 10.1373/clinchem.2003.026161

Sucher, N. J., Deitcher, D. L., Baro, D. J., Warrick, R. M., and Guenther, E. (2000). Genes and channels: patch/voltage-clamp analysis and single-cell RT-PCR. *Cell Tissue Res.* 302, 295–307. doi: 10.1007/s004410000289

Thakor, D. K., Lin, A., Matsuka, Y., Meyer, E. M., Ruangsri, S., Nishimura, I., et al. (2009). Increased peripheral nerve excitability and local NaV1.8 mRNA up-regulation in painful neuropathy. *Mol. Pain* 5:14. doi: 10.1186/1744-8069-5-14

Vijayaragavan, K., O'Leary, M. E., and Chahine, M. (2001). Gating properties of Na$_v$1.7 and Na$_v$1.8 peripheral nerve sodium channels. *J. Neurosci.* 21, 7909–7918.

Winlove, C. I., and Roberts, A. (2012). The firing patterns of spinal neurons: *in situ* patch-clamp recordings reveal a key role for potassium currents. *Eur. J. Neurosci.* 36, 2926–2940. doi: 10.1111/j.1460-9568.2012.08208.x

Xie, W., Strong, J. A., Ye, L., Mao, J. X., and Zhang, J. M. (2013). Knockdown of sodium channel NaV1.6 blocks mechanical pain and abnormal bursting activity of afferent neurons in inflamed sensory ganglia. *Pain* 154, 1170–1180. doi: 10.1016/j.pain.2013.02.027

Zhang, X. Y., Wen, J., Yang, W., Wang, C., Gao, L., Zheng, L. H., et al. (2013). Gain-of-function mutations in SCN11A cause familial episodic pain. *Am. J. Hum. Genet.* 93, 957–966. doi: 10.1016/j.ajhg.2013.09.016

Conflict of Interest Statement: The authors declare that the research was conducted in the absence of any commercial or financial relationships that could be construed as a potential conflict of interest.